Letter

Theoretical hyperfine splittings of $^{7,9}Be^{2+}$ ions for future studies of nuclear properties

Xiao-Qiu Qi,[1,2] Pei-Pei Zhang,[2,4,*] Zong-Chao Yan,[3,2] Ting-Yun Shi,[2] G. W. F. Drake,[4] Ai-Xi Chen,[1] and Zhen-Xiang Zhong[2]

[1]*Key Laboratory of Optical Field Manipulation of Zhejiang Province and Physics Department of Zhejiang Sci-Tech University, Hangzhou 310018, China*

[2]*State Key Laboratory of Magnetic Resonance and Atomic and Molecular Physics, Wuhan Institute of Physics and Mathematics, Innovation Academy for Precision Measurement Science and Technology, Chinese Academy of Sciences, Wuhan 430071, China*

[3]*Department of Physics, University of New Brunswick, Fredericton, New Brunswick, Canada E3B 5A3*

[4]*Canterbury College and Department of Physics, University of Windsor, Windsor, Ontario, Canada N9B 3P4*

(Received 22 November 2022; accepted 3 January 2023; published 23 January 2023)

The hyperfine structures of the $2\,^3S_1$ and $2\,^3P_J$ states of $^7Be^{2+}$ and $^9Be^{2+}$ are investigated within the framework of the nonrelativistic quantum electrodynamics, including relativistic and radiative corrections up to order $m\alpha^6$. The uncertainties of the calculated hyperfine splittings are on the order of tens of ppm, and for $^9Be^{2+}$ our results improve the previous theoretical and experimental values by at least two orders of magnitude. The improved sensitivity of the hyperfine splittings of $^{7,9}Be^{2+}$ to the nuclear Zemach radius and electric quadrupole moment opens the way to future measurements to extract the atomic physics values of these two nuclear properties to an accuracy of 5% or better.

DOI: 10.1103/PhysRevA.107.L010802

I. INTRODUCTION

Helium and heliumlike ions are among the simplest atomic systems whose electronic structures can be calculated with high precision using the well-developed theoretical methods [1–7] of which the nonrelativistic quantum electrodynamics (NRQED) is the most effective approach for light atomic systems [8–11]. For the helium $2\,^3P_J$ fine-structure, for example, the NRQED-based calculation has achieved a precision of about 1.7 kHz, far exceeding all other theoretical methods that were based on Dirac-like formalism [12]. Experimentally, Clausen *et al.* [13] recently reported a much improved determination of the He $2\,^1S_0$ ionization energy at the level of 32 kHz, which is in good accord with theory. However, the derived experimental ionization energies of the $2\,^3S_1$ and $2\,^3P_J$ states are in disagreement with theoretical predictions by 6.5σ and 10σ, respectively. Li^+ is very similar to helium with a higher Z and its QED effect is more significant than helium. For the $2\,^3P_1$-$2\,^3P_2$ fine-structure interval, for example, the QED contribution of order $m\alpha^6$ and higher in Li^+ is a factor of 26 larger than helium [14]. The hyperfine splittings (hfs) of Li^+ were studied in our previous work using the NRQED theory [5]. The theoretical uncertainty is reduced to less than 100 kHz by a complete calculation of all the QED corrections up to $m\alpha^6$. The so-called Zemach radius, which is defined as the convolution of the electric charge and the magnetic moment distributions inside the nucleus, can be extracted by combining precision measurements [14]. The obtained Zemach radius for ^{7}Li is in good agreement with previous values, but the value for ^{6}Li disagrees with the nuclear physics one [15] by more than 6σ, indicating an anomalous nuclear structure for ^{6}Li.

The next low-Z atom in the periodic table is beryllium, which has many isotopes, including a one-neutron halo ^{11}Be and a two-neutron halo ^{14}Be [16–19]. With the exception of the stable ^{9}Be nucleus, all other isotopes are unstable and thus atomic spectroscopy at the single-atom limit provides a uniquely powerful probe of their nuclear properties. There are some spectroscopic measurements to explore Be nuclear structure [16,18,20–24]. Blachman and Lurio [20] measured the ^{9}Be hyperfine structure and determined the nuclear quadrupole moment. Using laser-fluorescence mass spectroscopy, Wineland *et al.* [21] measured the $^9Be^+$ hyperfine A constant and derived indirectly the proton-to-electron mass ratio and the bound electron g factor. Okada *et al.* [22] determined the ^{7}Be nuclear magnetic dipole moment to high precision by laser-microwave double-resonance spectroscopy. The nuclear charge radii of ^{7,9,10,11,12}Be were determined by Nörtershäuser *et al.* [16,18] using collinear laser spectroscopy. Puchalski *et al.* [25] calculated the hyperfine splittings of ^{9}Be using explicitly correlated Gaussian (ECG) functions and accurately extracted the nuclear quadrupole moment by combining the hyperfine structure measurements of Blachman and Lurio [20], although it was inconsistent with most of the previous determinations. However, for the ^{7}Be nucleus, only nuclear physics determinations of the nuclear quadrupole moment exist and there are noticeable differences between them, e.g., -6.11 fm^2 [26], $-5.50(48)$ fm^2, and $-4.68(28)$ fm^2 [27].

Here we choose the helium-like Be^{2+} isotopes and explore their nuclear properties for the following reasons. First, they are suitable candidates for laser spectroscopy measurements because the transition wavelength of $2\,^3S-2\,^3P$ is 372 nm

*zhangpei@wipm.ac.cn

[28], which is near to the visible region. Second, since Be^{2+} is a three-body system, the QED theory is relatively simpler than for neutral Be. Third, experimental work on Be^{2+} is sparse compared to helium and Li^{+}. Scholl *et al.* [28] measured the $1s2s\,^3S_1 - 1s2p\,^3P_J$ transition of the $^9Be^{2+}$ ion by applying the fast ion beam laser fluorescence method with an accuracy of 1 part in 10^8, which represents a three orders of magnitude improvement over previous measurements. The extracted fine and hyperfine splittings are accurate to the order of tens of ppm and a few parts in 10^3, respectively. Johnson *et al.* [29] calculated the $2\,^3P_J$ hfs of $^9Be^{2+}$ to four-figure accuracy using the relativistic configuration interaction method. With advances in experimental techniques, especially the emergence of new light sources with narrow linewidths in the XUV region [30–32], it is now possible to improve the measurement of Be^{2+} to a new level of accuracy.

The purpose of this paper is to present a systematic calculation of hyperfine splittings for the $2\,^3S_1$ and $2\,^3P_J$ states of the $^{7,9}Be^{2+}$ ions by including QED corrections up to order $m\alpha^6$. The possibility of determining the nuclear Zemach radius and the electric quadrupole moment of a Be isotope based on Be^{2+} spectroscopy will be discussed. The remaining part of the Letter is organized as follows. Section II outlines the basic theoretical framework. Section III details various QED contributions to the hfs of $2\,^3S_1$ and $2\,^3P_J$ states of $^{7,9}Be^{2+}$. Some discussion on the impact of nuclear properties on hfs is presented in Sec. IV. Finally, a summary is given in Sec. V. Atomic units (a.u.) are used unless otherwise stated.

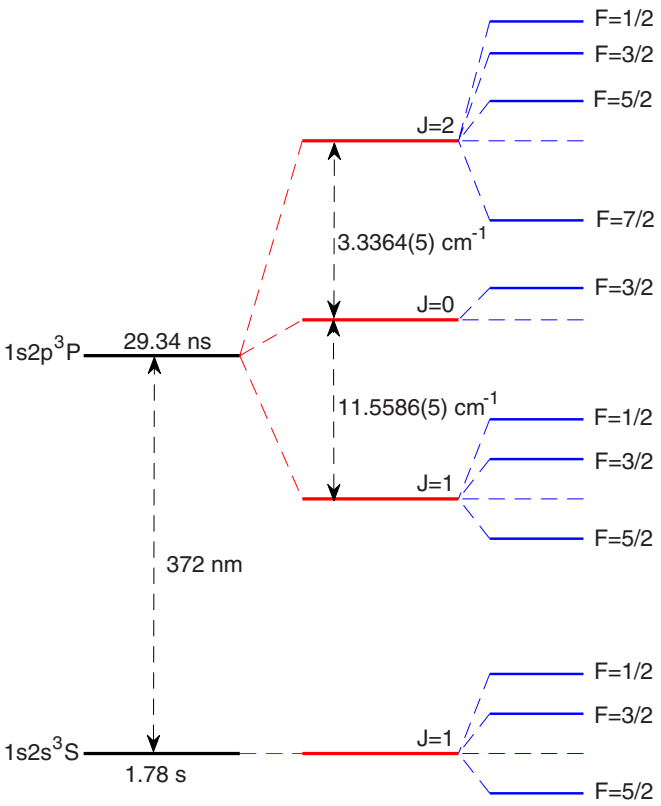

FIG. 1. Hyperfine energy levels (not to scale) of the $2\,^3S_1$ and $2\,^3P_J$ states of $^9Be^{2+}$.

II. THEORETICAL METHOD

The NRQED theory for quasidegenerate states was applied to calculate fine- and hyperfine structure splittings of light atomic systems [4,5,33–35]. Here we outline the framework for calculating relativistic and QED corrections to an energy level. Figure 1 shows the energy level diagram for $^9Be^{2+}$ (the diagram for $^7Be^{2+}$ is similar to $^9Be^{2+}$ since they have the same nuclear spin 3/2). The energies of the $2\,^3S_1$ and $2\,^3P_J$ states are obtained by diagonalizing the effective Hamiltonian H with matrix elements

$$E^F_{JJ'} \equiv \langle JFM_F|H|J'FM_F\rangle, \tag{1}$$

where M_F is the projection of the total angular momentum F, which can be fixed arbitrarily since the energies are independent of it. For convenience, we take the $2\,^3P_J$ centroid as the reference point. The above matrix elements Eq. (1) can be expanded in powers of the fine-structure constant α,

$$\begin{aligned} E^F_{JJ'} = {} & \langle H_{\rm fs}\rangle_J \delta_{JJ'} + \langle H^{(4+)}_{\rm hfs}\rangle + \langle H^{(6)}_{\rm hfs}\rangle \\ & + 2\langle H^{(4)}_{\rm hfs}, [H^{(4)}_{\rm nfs} + H^{(4)}_{\rm fs}]\rangle + \langle H^{(4)}_{\rm hfs}, H^{(4)}_{\rm hfs}\rangle \\ & + \langle H^{(6)}_{\rm QED}\rangle + \langle H^{\rm ho}_{\rm QED}\rangle + \langle H_{\rm nucl}\rangle + \langle H_{\rm eqm}\rangle, \end{aligned} \tag{2}$$

where $\langle A, B\rangle \equiv \langle A \frac{1}{(E_0 - H_0)'} B\rangle$, with H_0 and E_0 being the nonrelativistic Hamiltonian and its eigenvalue. $H_{\rm fs}$ is the effective operator that does not depend on the nuclear spin and is responsible for the fine-structure splittings [12,36]. All other terms in Eq. (2) are nuclear spin-dependent contributions. $H^{(4)}_{\rm hfs}$ is the leading-order hyperfine Hamiltonian of $m\alpha^4$ and $H^{(4+)}_{\rm hfs}$ is $H^{(4)}_{\rm hfs}$ with the higher-order terms from the recoil and anomalous magnetic moment effects included. $H^{(6)}_{\rm hfs}$ is the effective operator for the hyperfine splittings of order $m\alpha^6$. $H^{(4)}_{\rm fs}$ and $H^{(4)}_{\rm nfs}$ are the Breit Hamiltonians of order $m\alpha^4$ with and without electron spin. The fifth term in Eq. (2) is the second-order hyperfine correction, which contributes to the isotope shift, and fine and hyperfine splittings. $H^{(6)}_{\rm QED}$ and $H^{\rm ho}_{\rm QED}$ are the two effective operators for the QED corrections of order $m\alpha^6$ and higher $\sim m\alpha^7$. Finally, $H_{\rm nucl}$ and $H_{\rm eqm}$ represent the nuclear effects due to the Zemach radius and the nuclear electric quadrupole moment.

We solve the eigenvalue problem of H_0 variationally in Hylleraas coordinates. The relativistic and QED corrections, as well as the corrections due to nuclear structure, are evaluated perturbatively. The Hylleraas basis set [37] is constructed according to

$$\psi_{\ell mn}(\vec{r}_1, \vec{r}_2) = r_1^\ell r_2^m r^n e^{-\alpha r_1 - \beta r_2 - \gamma r} \mathcal{Y}^{LM}_{\ell_1\ell_2}(\hat{r}_1, \hat{r}_2), \tag{3}$$

where $\vec{r} = \vec{r}_1 - \vec{r}_2$ and $\mathcal{Y}^{LM}_{\ell_1\ell_2}(\hat{r}_1, \hat{r}_2)$ is the vector-coupled product of spherical harmonics for the two electrons. The mass polarization operator due to finite nuclear mass is included explicitly in the Hamiltonian for all terms in Eq. (2) except for the small second-order terms, and $\langle H_{\rm fs}\rangle$, which is determined from the experiment. The rate of convergence of some of the second-order terms can be greatly accelerated by including in the pseudostate basis sets terms that are more singular by an additional factor of $1/r_1$ or $1/r_2$ [38]. These terms do not contribute to the nonrelativistic wave function, but they do contribute to the solution to the corresponding perturbation equation. The necessary angular momentum

TABLE I. Expectation values of hfs operators for the $2\,^3S_1$ and $2\,^3P_J$ states of $^7Be^{2+}$ and $^9Be^{2+}$. The listed numerical values are uncertain only at the last digits. In atomic units.

State	Operator	$^7Be^{2+}$	$^9Be^{2+}$
$2\,^3S_1$	$4\pi\delta^3(\vec{r}_1)$	137.731960	137.739110
	K'	−157.232037	−157.232037
$2\,^3P_J$	$4\pi\delta^3(\vec{r}_1)$	126.232881	126.239606
	$(\vec{r}_1\times\vec{p}_1)/r_1^3$	1.814143	1.814146
	$(\vec{r}_1\times\vec{p}_2)/r_1^3$	−2.602150	−2.602181
	$(\delta^{ij}-3r_1^ir_1^j/r_1^2)/r_1^3$	−0.671762	−0.671769
	K'	55.3670854	55.3670854
	$\vec{K}$	−145.86034	−145.86034
	$\hat{K}$	−82.07829	−82.07829

operators, which can be evaluated analytically [5,34], are S^iL^i, I^iL^i, I^iS^i, $\{S^iS^j\}\{L^iL^j\}$, $I^iS^j\{L^iL^j\}$, $I^iL^j\{S^iS^j\}$, $\{I^iI^j\}\{S^iS^j\}$, $\{I^iI^j\}\{L^iL^j\}$, $\{I^iI^j\}L^iS^j$, and $\{I^iI^j\}[\{S^mS^n\}\{L^kL^l\}]^{ij}$, where $\{S^iS^j\}\equiv\frac{1}{2}S^iS^j+\frac{1}{2}S^jS^i-\frac{1}{3}\vec{S}^2\delta^{ij}$ and the summation over repeated indices is assumed.

III. HFS OF $2\,^3S_1$ AND $2\,^3P_J$ STATES

The hyperfine structure operators responsible for relativistic and QED corrections to the $2\,^3S_1$ and $2\,^3P_J$ states of helium-like ions are defined in our previous Ref. [5] and the present Supplemental Material [39]. Table I lists the results of first-order perturbation for the $m\alpha^4$ and $m\alpha^6$ operators.

The second-order corrections of $m\alpha^6$ can be divided into several parts according to the symmetries of the intermediate states. For the $2\,^3S_1$ state, the intermediate states are ^3S, ^3P, ^3D, and ^1S, whereas for $2\,^3P_J$ they are ^3P, ^1P, ^3D, ^1D, and ^3F. Numerical results of various operators for the radial parts are presented in Table II. Since the second-order hyperfine correction $\langle H^{(4)}_{\rm hfs}, H^{(4)}_{\rm hfs}\rangle$ is divergent, we calculate only the dominant contribution from the $2\,^1P_1$ intermediate state. Here the uncertainty of $\langle P_A, P_A\rangle^\circ$ in Table II is only computational. We also use the method in Ref. [34] to estimate the uncertainty due to this approximation, i.e., calculate the second-order perturbation of $\langle P'_A, P'_A\rangle$, and then take the difference between $\langle P_A, P_A\rangle^\circ$ and $\langle P'_A, P'_A\rangle$ as the uncertainty, which is 10 000 a.u. for $2\,^3S_1$ and 15 000 a.u. for $2\,^3P_J$. This translates into uncertainties of less than 2×10^{-10} cm^{-1} in the hfs.

We calculate the hfs of the $2\,^3S_1$ and $2\,^3P_J$ states using the values in Tables I and II. The contribution from the higher-order QED corrections is calculated from the weighted average [40,41]

$$H^{\rm ho}_{\rm QED}(1s2\ell)=\frac{H^{\rm ho}_{\rm QED}(1s)+H^{\rm ho}_{\rm QED}(2\ell)/8}{1+\delta_{\ell,0}/8}, \tag{4}$$

with $\ell=0,1$ for $2s$, $2p$, respectively. The uncertainty of the contribution is estimated as 20% of the contribution. According to Eq. (2), the hfs calculation of the $2\,^3P_J$ state requires the fine-structure splittings, which are $\langle H_{\rm fs}\rangle_{J=0}=(8f_{01}+5f_{12})/9$, $\langle H_{\rm fs}\rangle_{J=1}=(-f_{01}+5f_{12})/9$, and $\langle H_{\rm fs}\rangle_{J=2}=(-f_{01}-4f_{12})/9$, relative to the $2\,^3P_J$ centroid, with $f_{01}=11.5586(5)$ cm^{-1} and $f_{12}=-14.8950(4)$ cm^{-1} for $^9Be^{2+}$ [28]. The fine-structure splittings of $^7Be^{2+}$ are obtained by changing the reduced mass accordingly i.e., $f_{01}=11.558(2)$ cm^{-1} and $f_{12}=-14.895(2)$ cm^{-1}. In our calculations, the nuclear magnetic dipole moments are

TABLE II. Second-order matrix elements for all possible intermediate states connected to the $2\,^3S_1$ and $2\,^3P_J$ states. The listed numerical values are uncertain only at the last digits when not given explicitly. In atomic units.

State	Symmetry	$\langle A, B\rangle$	Value
$2\,^3S_1$	^3S	$\langle P', G'\rangle$	4592.8
	^3P	$\langle\vec{P},\vec{G}\rangle$	0.140
	^3D	$\langle\hat{P},\hat{G}\rangle$	0.87
	^1S	$\langle P_A, P_A\rangle^\circ$	−839 249.282
		$\langle P'_A, P'_A\rangle$	−848 800(200)
$2\,^3P_J$	^3P	$\langle P', G'\rangle$	4024.6(5)
		$\langle\vec{P}, G\rangle$	86.9(5)
		$\langle\hat{P}, G\rangle$	40(5)
		$\langle P,\vec{G}\rangle$	26.678
		$\langle\vec{P},\vec{G}\rangle$	−64.1
		$\langle\hat{P},\vec{G}\rangle$	−39.8427
		$\langle P,\hat{G}\rangle$	6.714(5)
		$\langle\vec{P},\hat{G}\rangle$	19.323
		$\langle\hat{P},\hat{G}\rangle$	8.882
	^1P	$\langle P_A,\vec{G}_A\rangle$	9054.88(5)
		$\langle P_A,\vec{G}_A\rangle^\circ$	9021.158
		$\langle\hat{P}_A,\vec{G}_A\rangle$	−176.7(5)
		$\langle\hat{P}_A,\vec{G}_A\rangle^\circ$	−139.044
		$\langle P_A, P_A\rangle^\circ$	−1 785 103.485
		$\langle P'_A, P'_A\rangle$	−1 797 300(200)
		$\langle P_A,\hat{P}_A\rangle^\circ$	27 527.773
		$\langle\hat{P}_A,\hat{P}_A\rangle^\circ$	−2547.006
	^3D	$\langle\vec{P},\vec{G}\rangle$	0.044
		$\langle\hat{P},\vec{G}\rangle$	−0.0149824
		$\langle\vec{P},\hat{G}\rangle$	1.563(5)
		$\langle\hat{P},\hat{G}\rangle$	–0.0688
	^1D	$\langle\hat{P}_A,\vec{G}_A\rangle$	0.348(5)
	^3F	$\langle\hat{P},\hat{G}\rangle$	0.628(5)

TABLE III. Theoretical values for individual $2\,^3S_1$ and $2\,^3P_J$ energy levels in $^7Be^{2+}$ and $^9Be^{2+}$, relative to the $2\,^3S_1$ and $2\,^3P_J$ centroid, where the first error in $2\,^3P$ is due to the fine structure and the second is due to the hyperfine structure, in cm^{-1}.

State	(J, F)	$^7Be^{2+}$	$^9Be^{2+}$
$2\,^3S$	(1, 1/2)	0.68251(1)	0.574282(6)
	(1, 3/2)	0.27300(1)	0.229708(3)
	(1, 5/2)	−0.40950(1)	−0.344566(4)
$2\,^3P$	(2, 1/2)	5.90767(100)(1)	5.817172(190)(6)
	(2, 3/2)	5.72041(100)(1)	5.658805(190)(4)
	(2, 5/2)	5.40467(100)(1)	5.392683(190)(1)
	(2, 7/2)	4.95513(100)(1)	5.015548(190)(4)
	(0, 3/2)	2.01174(200)(1)	2.008479(500)(1)
	(1, 1/2)	−9.23556(110)(1)	−9.287087(230)(3)
	(1, 3/2)	−9.44648(110)(1)	−9.461891(230)(1)
	(1, 5/2)	−9.75933(110)(1)	−9.727037(230)(2)

TABLE IV. Calculated values of $^7Be^{2+}$ and $^9Be^{2+}$ hfs coefficients for the $2\,^1P_1$ and $2\,^3P_J$ states, in cm^{-1}. These coefficients are defined in Eqs. (10) to (12) of Ref. [36]. The listed numerical values are uncertain only at the last digits.

Coefficient	$^7Be^{2+}$	$^9Be^{2+}$
$C^{(0)}_{1,1}$	−0.24990	−0.210283
$C^{(0)}_{1,0}$	−0.25126	−0.211428
$D^{(0)}_{1}$	−0.00440	−0.003701
$D^{(0)}_{0}$	−0.00317	−0.002663
$E^{(0)}_{1,1}$	0.00112	0.000938
$E^{(0)}_{1,0}$	0.00097	0.000815

$-1.39928(2)\,\mu_N$ [22] and $-1.177432(3)\,\mu_N$ [16] and the nuclear quadrupole moments are $-6.11\,fm^2$ (the theoretical value from Ref. [26]) and $5.350(14)\,fm^2$ [25] for $^7Be^{2+}$ and $^9Be^{2+}$, respectively. The Zemach radius of ^9Be is 4.07(5) fm derived from a comparison between the theory and experiment of the lithiumlike $^9Be^+$ [25]. For ^7Be it is 3.45(11) fm, which is estimated by $R_{em} = 4R_e/\sqrt{3\pi}$ using the Gaussian distribution [36] and $R_e = 2.647(17)$ fm is the nuclear charge radius [16]. To be conservative, we choose five times the uncertainty from R_e as the error in R_{em}. The hyperfine levels of $2\,^3S_1$ and $2\,^3P_J$ states can be obtained by diagonalizing the matrix formed by Eq. (2) and the results relative to the $2\,^3S_1$ and $2\,^3P_J$ centroids are listed in Table III.

Singlet-triplet mixing for the $n = 2$ manifold of P states eventually becomes saturated with increasing Z, and so should be treated by exact diagonalization [5,39] instead of second-order perturbation theory. To check the effect for $Z = 4$, we compared the results of a restricted diagonalization within the $2\,^3P_J$ manifold of hyperfine states (method 1), with the results of an extended diagonalization that includes also the $2\,^1P_J$ hyperfine states (method 2). Both the methods include the relativistic corrections of order $m\alpha^4$. The second-order matrix elements and the hyperfine structure coefficients [36] for the $2\,^1P_1$ and $2\,^3P_J$ states are listed in Tables II and IV as inputs. The hfs of $2\,^3P_J$ obtained by both methods is compared in Table V. The extended diagonalization (method 2) alters the hyperfine intervals $(1, 1/2) - (1, 3/2)$ and $(1, 3/2) - (1, 5/2)$ by 0.000322 cm^{-1} and 0.000516 cm^{-1} for $^9Be^{2+}$, whereas for $^7Be^{2+}$ they are 0.00038 cm^{-1} and 0.00061 cm^{-1}, respectively. These shifts are about three orders of magnitude larger than for the case of $^7Li^+$ with $Z = 3$. Our final results

TABLE V. Hyperfine splittings in $2\,^3P_J$ of $^7Be^{2+}$ and $^9Be^{2+}$, in cm^{-1}. Only the relativistic correction of order $m\alpha^4$ is included. The listed numerical values are uncertain only at the last digits.

	$(J, F) - (J', F')$	Method 1	Method 2	Difference
$^7Be^{2+}$	$(2, 1/2) - (2, 3/2)$	0.18729	0.18729	
	$(2, 3/2) - (2, 5/2)$	0.31552	0.31552	
	$(2, 5/2) - (2, 7/2)$	0.44873	0.44872	−0.00001
	$(1, 1/2) - (1, 3/2)$	0.21031	0.21069	0.00038
	$(1, 3/2) - (1, 5/2)$	0.31267	0.31328	0.00061
$^9Be^{2+}$	$(2, 1/2) - (2, 3/2)$	0.157960	0.157964	0.000004
	$(2, 3/2) - (2, 5/2)$	0.265658	0.265660	0.000002
	$(2, 5/2) - (2, 7/2)$	0.376899	0.376891	−0.000008
	$(1, 1/2) - (1, 3/2)$	0.174864	0.175186	0.000322
	$(1, 3/2) - (1, 5/2)$	0.264669	0.265185	0.000516

of $2\,^3S_1$ and $2\,^3P_J$ hfs for $^7Be^{2+}$ and $^9Be^{2+}$ are shown in Tables VI and VII (see more discussion below), respectively.

IV. DISCUSSIONS

The Zemach radius R_{em} has a linear effect on hfs of $2\,^3S_1$ state

$$\nu = \nu_0 + CR_{em}, \tag{5}$$

where ν is the hfs between two hyperfine levels, ν_0 is the hfs without the contribution from the Zemach term, and C is the coefficient independent of R_{em}. Then we have

$$\left|\frac{\delta\nu}{\nu}\right| = \zeta\left|\frac{\delta R_{em}}{R_{em}}\right|, \tag{6}$$

where ζ is the sensitivity coefficient defined by

$$\zeta = \left|\frac{CR_{em}}{\nu}\right|, \tag{7}$$

and can be approximated by $2ZR_{em}/a_0$ with a_0 being the Bohr radius [5]. To our knowledge, there is no experimental determination for the ^7Be Zemach radius. Here we use $R_{em} = 3.45(11)$ fm for ^7Be and $R_{em} = 4.07(5)$ fm for ^9Be as mentioned above. Using Eq. (2), the final calculated results of hfs and the contribution of the Zemach radius for the $2\,^3S_1$ state are listed in Table VI. For $^9Be^{2+}$, our results are not only consistent with the experimental values of Scholl *et al.* [28], but are at least two orders of magnitude more precise. It is

TABLE VI. Theoretical hyperfine intervals in the $2\,^3S_1$ state of $^7Be^{2+}$ and $^9Be^{2+}$ with the Zemach radius $R_{em} = 3.45(11)$ fm and $R_{em} = 4.07(5)$ fm, respectively.

	$(J, F) - (J', F')$	ν_0 cm^{-1}	10^5C cm^{-1}/fm	ν (This work) cm^{-1}	Scholl *et al.* [28] cm^{-1}	ζ ppm	$\lvert\delta R_{em}/R_{em}\rvert$ %
$^7Be^{2+}$	$(1, 1/2) - (1, 3/2)$	0.40973(1)	−6.189	0.40952(1) at 24 ppm		521(17)	5
	$(1, 3/2) - (1, 5/2)$	0.68286(1)	−10.315	0.68250(1) at 15 ppm		521(17)	3
$^9Be^{2+}$	$(1, 1/2) - (1, 3/2)$	0.344786(8)	−5.208	0.344574(9) at 26 ppm	0.3448(10)	615(8)	4
	$(1, 3/2) - (1, 5/2)$	0.574628(5)	−8.680	0.574275(6) at 10 ppm	0.5740(11)	615(8)	2

TABLE VII. Theoretical hyperfine intervals in the $2\,^3P_J$ state of $^7Be^{2+}$ and $^9Be^{2+}$ with the nuclear quadrupole moments $Q_d = -6.11\,\mathrm{fm}^2$ and $Q_d = 5.350(14)\,\mathrm{fm}^2$, respectively.

	$(J,F)-(J',F')$	$\nu(0)$ cm^{-1}	10^5X $\mathrm{cm}^{-1}/\mathrm{fm}^2$	$\nu(Q_d)$ (This work) cm^{-1}	Johnson *et al.* [29] cm^{-1}	Scholl *et al.* [28] cm^{-1}	η ppm	$\lvert\delta Q_d/Q_d\rvert$ %
$^7Be^{2+}$	$(2,1/2)-(2,3/2)$	0.18751(1)	4.1501	0.18726(1) at 53 ppm			1400	4
	$(2,3/2)-(2,5/2)$	0.31591(1)	2.7393	0.31574(1) at 32 ppm			600	5
	$(2,5/2)-(2,7/2)$	0.44928(1)	−4.0189	0.44953(1) at 22 ppm			600	4
	$(1,1/2)-(1,3/2)$	0.21097(1)	−5.3409	0.21130(1) at 47 ppm			1500	3
	$(1,3/2)-(1,5/2)$	0.31365(1)	3.1606	0.31346(1) at 32 ppm			600	5
$^9Be^{2+}$	$(2,1/2)-(2,3/2)$	0.158149(7)	4.1472	0.158371(7) at 44 ppm	0.1581	0.1585(10)	1400	3
	$(2,3/2)-(2,5/2)$	0.265975(4)	2.7698	0.266123(4) at 15 ppm	0.2659	0.2659(11)	600	3
	$(2,5/2)-(2,7/2)$	0.377344(4)	−4.0349	0.377128(4) at 11 ppm	0.3773	0.3768(14)	600	2
	$(1,1/2)-(1,3/2)$	0.175411(4)	−5.3343	0.175126(4) at 23 ppm	0.1754	0.1751(10)	1600	1
	$(1,3/2)-(1,5/2)$	0.265495(3)	3.1266	0.265662(3) at 11 ppm	0.2654	0.2654(10)	600	2

noted that the uncertainties in our theoretical values of about 10–26 ppm are mainly caused by the nuclear magnetic dipole moments. The last column in the table is the predicted accuracy of R_{em} estimated according to Eq. (6) using the listed sensitivity coefficients ζ. In other words, once the accuracy of future experiments reaches the level of around 25 ppm or better, we can extract an atomic physics value of the Zemach radius of ^{7}Be or ^{9}Be with an uncertainty of about 5% or better.

Next, we study the influence of the quadrupole moment Q_d on the hfs of $2\,^3P_J$ state by Taylor expanding the transition frequency $\nu(Q_d)$ between two hyperfine levels at $Q_d = 0$:

$$\nu(Q_d) = \nu(0) + XQ_d + O\big(Q_d^2\big), \tag{8}$$

where $\nu(0)$ is the hfs obtained by diagonalization of Eq. (2) without Q_d, i.e., without the H_{eqm} term and X is the linear expansion coefficient independent of Q_d that can be evaluated through the first-order derivative of $\nu(Q_d)$ at $Q_d = 0$. In the above expansion, the quadratic term and beyond in Q_d are too small to be significant. Then we haves

$$\left|\frac{\delta\nu(Q_d)}{\nu(Q_d)}\right| = \eta\left|\frac{\delta Q_d}{Q_d}\right|, \tag{9}$$

where η is the sensitivity coefficient defined by

$$\eta = \left|\frac{XQ_d}{\nu(Q_d)}\right|. \tag{10}$$

Using the value $Q_d = -6.11\,\mathrm{fm}^2$ from Ref. [26] for ^{7}Be and $Q_d = 5.350(14)\,\mathrm{fm}^2$ from Ref. [25] for ^{9}Be, our calculated results for $\nu(0)$, X, $\nu(Q_d)$, and η are listed in Table VII. The uncertainties of our theoretical calculations are in the range of about 10–50 ppm. For $^7Be^{2+}$, the uncertainties in our theoretical hfs are mainly from the nuclear magnetic dipole moment, the Zemach radius, and the $m\alpha^7$ QED effect. For $^9Be^{2+}$, the main sources of errors are from the $m\alpha^7$ QED effect and the Zemach radius; the error from the nuclear magnetic dipole moment becomes less significant due to the fact that it is more precise than $^7Be^{2+}$ by a factor of 5. Furthermore, the uncertainties from the fine structure are canceled for the same-J transitions. For $^9Be^{2+}$, Table VII also shows the measured results obtained by the weighted average of all the values in Ref. [28], as well as the only available theoretical calculations of Johnson *et al.* [29]. Our results are in good agreement with these previous results and are at least two orders of magnitude more precise. From the sensitivity coefficient η in Table VII we can see that the most sensitive transitions to Q_d are $(1,1/2)-(1,3/2)$ and $(2,1/2)-(2,3/2)$ for both $^7Be^{2+}$ and $^9Be^{2+}$. The last column in the table is the predicted accuracy of Q_d estimated according to Eq. (9), which we could extract once future measurements reach the current theoretical accuracy.

V. SUMMARY

In summary, we studied the hyperfine structure of the $2\,^3S_1$ and $2\,^3P_J$ states of $^{7,9}Be^{2+}$ ions, including the relativistic and QED corrections up to order $m\alpha^6$. The $2\,^1P_1 - 2\,^3P_1$ singlet-triplet mixing effect was treated by exact diagonalization for $n = 2$ and by perturbation theory for the remainder. Compared to Li^+, the $2\,^1P_1 - 2\,^3P_1$ mixing effect is about three orders of magnitude larger, indicating that this procedure becomes essential with increasing Z. The uncertainties of the present calculations are on the order of tens of ppm, mainly from the higher-order QED correction of $m\alpha^7$ and nuclear structure contributions. Our results for the hyperfine splittings in the $2\,^3S_1$ and $2\,^3P_J$ states of $^9Be^{2+}$ have improved the previous measurements and calculations by at least two orders of magnitude. The sensitivity coefficients of the hyperfine splittings of $^{7,9}Be^{2+}$ to the nuclear Zemach radius and electric quadrupole moment have also been estimated. To extract the Zemach radius accurate to 5% or better, the necessary experimental precision should be around 25 ppm or better. For the nuclear quadrupole moment, a determination of 5% or better is possible once the experimental precision reaches 50 ppm or better. An atomic physics determination of these nuclear properties will have important implications for testing low-energy nuclear models, especially for the relatively poorly understood unstable ^{7}Be isotope. Finally, the present calculations can readily be extended to the one-neutron halo ^{11}Be isotope that has nuclear spin 1/2.

ACKNOWLEDGMENTS

This research was supported by the National Natural Science Foundation of China under Grants No. 12174400, No.

11974382, No. 12274423, No. 12204412, and No. 12175199, and the Science Foundation of Zhejiang Sci-Tech University under Grant No. 21062349-Y. Z.-C.Y. and G.W.F.D. acknowledge support from the Natural Sciences and Engineering Research Council of Canada (NSERC) and by the Digital Research Alliance of Canada/Compute Ontario.

[1] Z.-C. Yan and G. W. F. Drake, Phys. Rev. Lett. **74**, 4791 (1995).
[2] V. Patkóš, V. A. Yerokhin, and K. Pachucki, Phys. Rev. A **94**, 052508 (2016).
[3] V. Patkóš, V. A. Yerokhin, and K. Pachucki, Phys. Rev. A **95**, 012508 (2017).
[4] V. Patkóš, V. A. Yerokhin, and K. Pachucki, Phys. Rev. A **100**, 042510 (2019).
[5] X.-Q. Qi, P.-P. Zhang, Z.-C. Yan, G. W. F. Drake, Z.-X. Zhong, T.-Y. Shi, S.-L. Chen, Y. Huang, H. Guan, and K.-L. Gao, Phys. Rev. Lett. **125**, 183002 (2020).
[6] V. Patkóš, V. A. Yerokhin, and K. Pachucki, Phys. Rev. A **103**, 042809 (2021).
[7] V. Patkóš, V. A. Yerokhin, and K. Pachucki, Phys. Rev. A **103**, 012803 (2021).
[8] K. Pachucki, U. D. Jentschura, and V. A. Yerokhin, Phys. Rev. Lett. **93**, 150401 (2004).
[9] K. Pachucki, U. D. Jentschura, and V. A. Yerokhin, Phys. Rev. Lett. **94**, 229902 (2005).
[10] U. D. Jentschura, A. Czarnecki, and K. Pachucki, Phys. Rev. A **72**, 062102 (2005).
[11] K. Pachucki, V. Patkóš, and V. A. Yerokhin, Phys. Rev. A **95**, 062510 (2017).
[12] K. Pachucki and V. A. Yerokhin, Phys. Rev. Lett. **104**, 070403 (2010).
[13] G. Clausen, P. Jansen, S. Scheidegger, J. A. Agner, H. Schmutz, and F. Merkt, Phys. Rev. Lett. **127**, 093001 (2021).
[14] H. Guan, S. Chen, X.-Q. Qi, S. Liang, W. Sun, P. Zhou, Y. Huang, P.-P. Zhang, Z.-X. Zhong, Z.-C. Yan, G. W. F. Drake, T.-Y. Shi, and K. Gao, Phys. Rev. A **102**, 030801(R) (2020).
[15] V. A. Yerokhin, Phys. Rev. A **78**, 012513 (2008).
[16] W. Nörtershäuser, D. Tiedemann, M. Žáková, Z. Andjelkovic, K. Blaum, M. L. Bissell, R. Cazan, G. W. F. Drake, C. Geppert, M. Kowalska, J. Krämer, A. Krieger, R. Neugart, R. Sánchez, F. Schmidt-Kaler, Z.-C. Yan, D. T. Yordanov, and C. Zimmermann, Phys. Rev. Lett. **102**, 062503 (2009).
[17] H. T. Fortune and R. Sherr, Phys. Rev. C **85**, 051303 (2012).
[18] A. Krieger, K. Blaum, M. L. Bissell, N. Frömmgen, C. Geppert, M. Hammen, K. Kreim, M. Kowalska, J. Krämer, T. Neff, R. Neugart, G. Neyens, W. Nörtershäuser, C. Novotny, R. Sánchez, and D. T. Yordanov, Phys. Rev. Lett. **108**, 142501 (2012).
[19] M. Labiche, F. M. Marqués, O. Sorlin, and N. Vinh Mau, Phys. Rev. C **60**, 027303 (1999).
[20] A. G. Blachman and A. Lurio, Phys. Rev. **153**, 164 (1967).
[21] D. J. Wineland, J. J. Bollinger, and W. M. Itano, Phys. Rev. Lett. **50**, 628 (1983).
[22] K. Okada, M. Wada, T. Nakamura, A. Takamine, V. Lioubimov, P. Schury, Y. Ishida, T. Sonoda, M. Ogawa, Y. Yamazaki, Y. Kanai, T. M. Kojima, A. Yoshida, T. Kubo, I. Katayama, S. Ohtani, H. Wollnik, and H. A. Schuessler, Phys. Rev. Lett. **101**, 212502 (2008).
[23] Z.-T. Lu, P. Mueller, G. W. F. Drake, W. Nörtershäuser, S. C. Pieper, and Z.-C. Yan, Rev. Mod. Phys. **85**, 1383 (2013).
[24] W. Nörtershäuser, C. Geppert, A. Krieger, K. Pachucki, M. Puchalski, K. Blaum, M. L. Bissell, N. Frömmgen, M. Hammen, M. Kowalska, J. Krämer, K. Kreim, R. Neugart, G. Neyens, R. Sánchez, and D. T. Yordanov, Phys. Rev. Lett. **115**, 033002 (2015).
[25] M. Puchalski, J. Komasa, and K. Pachucki, Phys. Rev. Res. **3**, 013293 (2021).
[26] A. Koji, O. Yoko, S. Yasuyuki, and V. Kálmán, Prog. Theor. Phys. Suppl. **142**, 97 (2001).
[27] C. Forssén, E. Caurier, and P. Navrátil, Phys. Rev. C **79**, 021303 (2009).
[28] T. J. Scholl, R. Cameron, S. D. Rosner, L. Zhang, R. A. Holt, C. J. Sansonetti, and J. D. Gillaspy, Phys. Rev. Lett. **71**, 2188 (1993).
[29] W. R. Johnson, K. T. Cheng, and D. R. Plante, Phys. Rev. A **55**, 2728 (1997).
[30] R. J. Jones, K. D. Moll, M. J. Thorpe, and J. Ye, Phys. Rev. Lett. **94**, 193201 (2005).
[31] A. Cingöz, D. C. Yost, T. K. Allison, A. Ruehl, M. E. Fermann, I. Hartl, and J. Ye, Nature (London) **482**, 68 (2012).
[32] J. Zhang, L.-Q. Hua, Z. Chen, M.-F. Zhu, C. Gong, and X.-J. Liu, Chin. Phys. Lett. **37**, 124203 (2020).
[33] M. Puchalski and K. Pachucki, Phys. Rev. A **79**, 032510 (2009).
[34] K. Pachucki, V. A. Yerokhin, and P. Cancio Pastor, Phys. Rev. A **85**, 042517 (2012).
[35] M. Haidar, Z.-X. Zhong, V. I. Korobov, and J.-P. Karr, Phys. Rev. A **101**, 022501 (2020).
[36] E. Riis, A. G. Sinclair, O. Poulsen, G. W. F. Drake, W. R. C. Rowley, and A. P. Levick, Phys. Rev. A **49**, 207 (1994).
[37] P.-P. Zhang, Z.-X. Zhong, Z.-C. Yan, and T.-Y. Shi, Chin. Phys. B **24**, 033101 (2015).
[38] G. W. F. Drake, Can. J. Phys. **80**, 1195 (2002).
[39] See Supplemental Material at http://link.aps.org/supplemental/10.1103/PhysRevA.107.L010802 for details of the formulas and numerical results, which includes Refs. [40–48].
[40] D. K. McKenzie and G. W. F. Drake, Phys. Rev. A **44**, R6973 (1991).
[41] Z.-C. Yan and G. W. F. Drake, Phys. Rev. A **61**, 022504 (2000).
[42] K. Pachucki, Phys. Rev. A **74**, 022512 (2006).
[43] K. Pachucki and V. A. Yerokhin, J. Phys. Chem. Ref. Data **44**, 031206 (2015).
[44] S. G. Karshenboim and V. G. Ivanov, Eur. Phys. J. D. **19**, 13 (2002).
[45] M. Puchalski and K. Pachucki, Phys. Rev. Lett. **111**, 243001 (2013).
[46] V. A. Yerokhin and K. Pachucki, Phys. Rev. A **81**, 022507 (2010).
[47] U. D. Jentschura and V. A. Yerokhin, Phys. Rev. A **81**, 012503 (2010).
[48] P. J. Mohr, B. N. Taylor, and D. B. Newell, Rev. Mod. Phys. **80**, 633 (2008).